A Search for correlations between turbulence and star formation in LITTLE THINGS dwarf irregular galaxies

Deidre A. Hunter[1], Bruce G. Elmegreen[2], Haylee Archer[1], Caroline E. Simpson[3], and Phil Cigan[4]

ABSTRACT

Turbulence has the potential for creating gas density enhancements that initiate cloud and star formation (SF), and it can be generated locally by SF. To study the connection between turbulence and SF, we looked for relationships between SF traced by FUV images, and gas turbulence traced by kinetic energy density (KED) and velocity dispersion (v_{disp}) in the LITTLE THINGS sample of nearby dIrr galaxies. We performed 2D cross-correlations between FUV and KED images, measured cross-correlations in annuli to produce correlation coefficients as a function of radius, and determined the cumulative distribution function of the cross correlation value. We also plotted on a pixel-by-pixel basis the locally excess KED, v_{disp}, and H I mass surface density, $\Sigma_{\rm HI}$, as determined from the respective values with the radial profiles subtracted, versus the excess SF rate density $\Sigma_{\rm SFR}$, for all regions with positive excess $\Sigma_{\rm SFR}$. We found that $\Sigma_{\rm SFR}$ and KED are poorly correlated. The excess KED associated with SF implies a $\sim 0.5\%$ efficiency for supernova energy to pump local H I turbulence on the scale of resolution here, which is a factor of ~ 2 too small for all of the turbulence on a galactic scale. The excess v_{disp} in SF regions is also small, only ~ 0.37 km s^{-1}. The local excess in $\Sigma_{\rm HI}$ corresponding to an excess in $\Sigma_{\rm SFR}$ is consistent with an H I consumption time of ~ 1.6 Gyr in the inner parts of the galaxies. The similarity between this timescale and the consumption time for CO implies that

Table 1. The Galaxy Sample

Galaxy	D[a] (Mpc)	M_V	$R_{H\alpha}$[b] (kpc)	$R_{FUVknot}$[c] (kpc)	R_D[d] (kpc)	R_{Br}[e] (kpc)	$\log SFR_D^{FUV}$[f] ($M_\odot$ yr^{-1} kpc^{-2})
CVnIdwA	3.6 ± 0.08	−12.37 ± 0.09	0.69	0.49±0.03	0.25±0.12	0.56±0.49	−1.77 ± 0.04
DDO 43	7.8 ± 0.8	−15.06 ± 0.22	2.36	1.93±0.08	0.87±0.10	1.46±0.53	−2.20 ± 0.04
DDO 46	6.1 ± 0.4	−14.67 ± 0.16	1.51	3.02±0.06	1.13±0.05	1.27±0.18	−2.45 ± 0.04
DDO 47	5.2 ± 0.6	−15.46 ± 0.24	5.58	5.58±0.05	1.34±0.05	···	−2.38 ± 0.04
DDO 50	3.4 ± 0.05	−16.61 ± 0.03	···	4.86±0.03	1.48±0.06	2.65±0.27	−1.81 ± 0.04
DDO 52	10.3 ± 0.8	−15.45 ± 0.17	3.69	3.39±0.10	1.26±0.04	2.80±1.35	−2.53 ± 0.04
DDO 53	3.6 ± 0.05	−13.84 ± 0.03	1.25	1.19±0.03	0.47±0.01	0.62±0.09	−1.96 ± 0.04
DDO 63	3.9 ± 0.05	−14.78 ± 0.03	2.26	2.89±0.04	0.68±0.01	1.31±0.10	−2.05 ± 0.04
DDO 69	0.8 ± 0.04	−11.67 ± 0.11	0.76	0.76±0.01	0.19±0.01	0.27±0.05	−2.22 ± 0.04
DDO 70	1.3 ± 0.07	−14.10 ± 0.12	1.23	1.34±0.01	0.44±0.01	0.13±0.07	−2.17 ± 0.04
DDO 75	1.3 ± 0.05	−13.91 ± 0.08	1.17	1.38±0.01	0.18±0.01	0.71±0.08	−0.99 ± 0.04
DDO 87	7.7 ± 0.5	−14.98 ± 0.15	3.18	4.23±0.07	1.21±0.02	0.99±0.11	−2.61 ± 0.04
DDO 101	6.4 ± 0.5	−15.01 ± 0.16	1.23	1.23±0.06	0.97±0.06	1.16±0.11	−2.84 ± 0.04
DDO 126	4.9 ± 0.5	−14.85 ± 0.24	2.84	3.37±0.05	0.84±0.13	0.60±0.05	−2.18 ± 0.04
DDO 133	3.5 ± 0.2	−14.75 ± 0.16	2.60	2.20±0.03	1.22±0.04	2.25±0.24	−2.60 ± 0.04
DDO 154	3.7 ± 0.3	−14.19 ± 0.16	1.73	2.65±0.04	0.48±0.02	0.62±0.09	−1.77 ± 0.04
DDO 167	4.2 ± 0.5	−12.98 ± 0.25	0.81	0.70±0.04	0.22±0.01	0.56±0.11	−1.59 ± 0.04
DDO 168	4.3 ± 0.5	−15.72 ± 0.25	2.24	2.25±0.04	0.83±0.01	0.72±0.07	−2.06 ± 0.04
DDO 187	2.2 ± 0.07	−12.68 ± 0.07	0.30	0.42±0.02	0.37±0.06	0.28±0.05	−2.60 ± 0.04
DDO 210	0.9 ± 0.04	−10.88 ± 0.10	···	0.29±0.01	0.16±0.01	···	−2.66 ± 0.04
DDO 216	1.1 ± 0.05	−13.72 ± 0.10	0.42	0.59±0.01	0.52±0.01	1.77±0.45	−3.17 ± 0.04
F564-V3	8.7 ± 0.7	−13.97 ± 0.18	···	1.24±0.08	0.63±0.09	0.73±0.40	−2.94 ± 0.04
IC 1613	0.7 ± 0.05	−14.60 ± 0.16	···	1.77±0.01	0.53±0.02	0.71±0.12	−1.97 ± 0.04
LGS 3	0.7 ± 0.08	−9.74 ± 0.25	···	0.32±0.01	0.16±0.01	0.27±0.08	−3.75 ± 0.04
M81dwA	3.6 ± 0.2	−11.73 ± 0.13	···	0.71±0.03	0.27±0.00	0.38±0.03	−2.30 ± 0.04
NGC 1569	3.4 ± 0.2	−18.24 ± 0.13	···	1.14±0.03	0.46±0.02	0.85±0.24	−0.32 ± 0.04
NGC 2366	3.4 ± 0.3	−16.79 ± 0.20	5.58	6.79±0.03	1.91±0.25	2.57±0.80	−2.04 ± 0.04
NGC 3738	4.9 ± 0.5	−17.12 ± 0.24	1.48	1.21±0.05	0.77±0.01	1.16±0.20	−1.52 ± 0.04
NGC 4163	2.9 ± 0.04	−14.45 ± 0.03	0.88	0.47±0.03	0.32±0.00	0.71±0.48	−1.89 ± 0.04
NGC 4214	3.0 ± 0.05	−17.63 ± 0.04	···	5.46±0.03	0.75±0.01	0.83±0.14	−1.11 ± 0.04
Sag DIG	1.1 ± 0.07	−12.46 ± 0.14	0.51	0.65±0.01	0.32±0.05	0.57±0.14	−2.40 ± 0.04
WLM	1.0 ± 0.07	−14.39 ± 0.15	1.24	2.06±0.01	1.18±0.24	0.83±0.16	−2.78 ± 0.04
Haro 29	5.8 ± 0.3	−14.62 ± 0.11	0.96	0.86±0.06	0.33±0.00	1.15±0.26	−1.21 ± 0.04
Haro 36	9.3 ± 0.6	−15.91 ± 0.15	1.06	1.79±0.09	1.01±0.00	1.16±0.13	−1.88 ± 0.04
Mrk 178	3.9 ± 0.5	−14.12 ± 0.26	1.17	1.45±0.04	0.19±0.00	0.38±0.00	−1.17 ± 0.04
VIIZw403	4.4 ± 0.07	−14.27 ± 0.04	1.27	0.33±0.04	0.53±0.02	1.02±0.29	−1.80 ± 0.04

- KED MAPS: $0.5 \times N_{HI} \times V^2$
- FUV images

Измеряют коэффициент корреляции в 2D

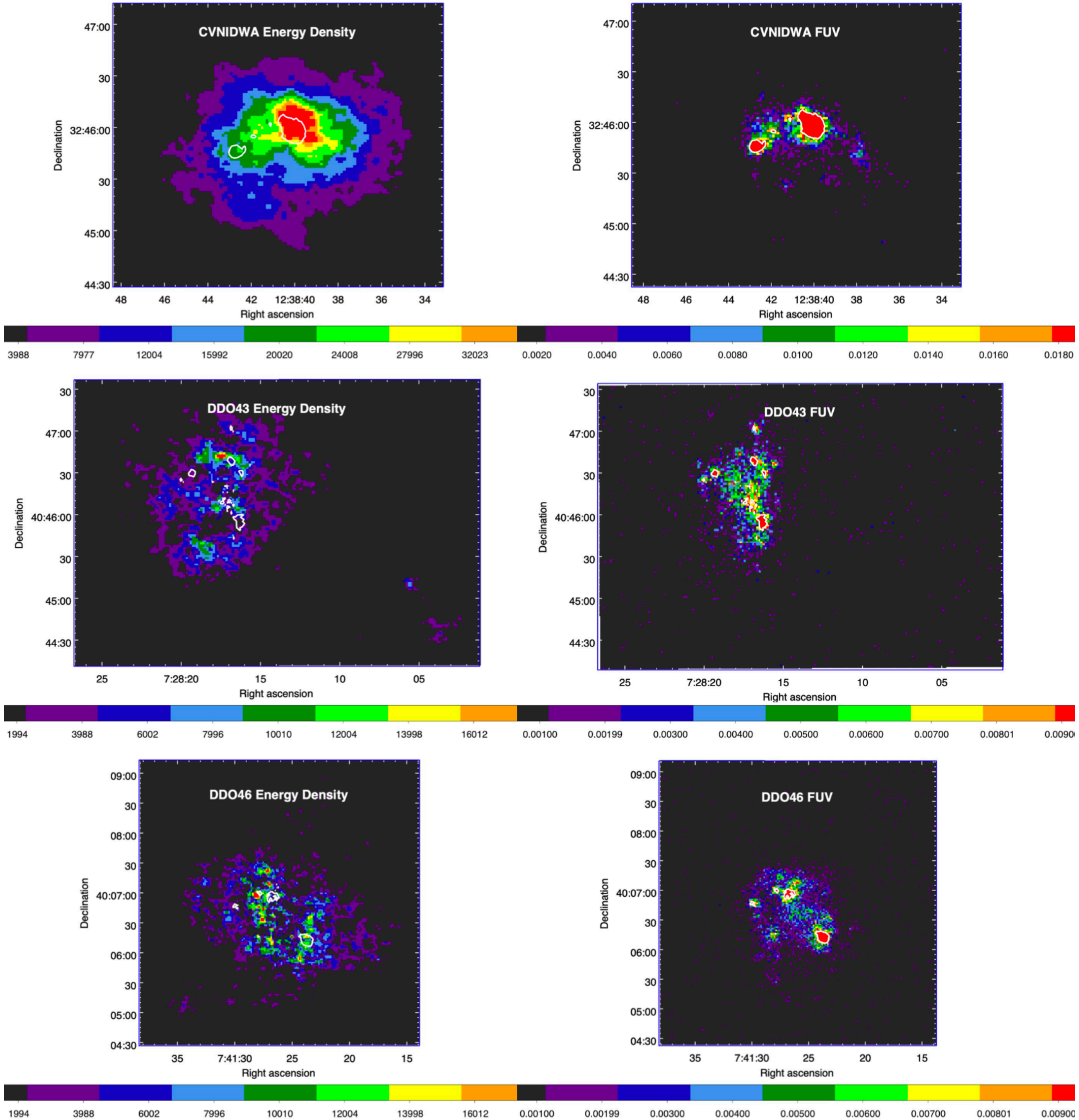

• Четкой корреляции

или антикорреляции они не видят

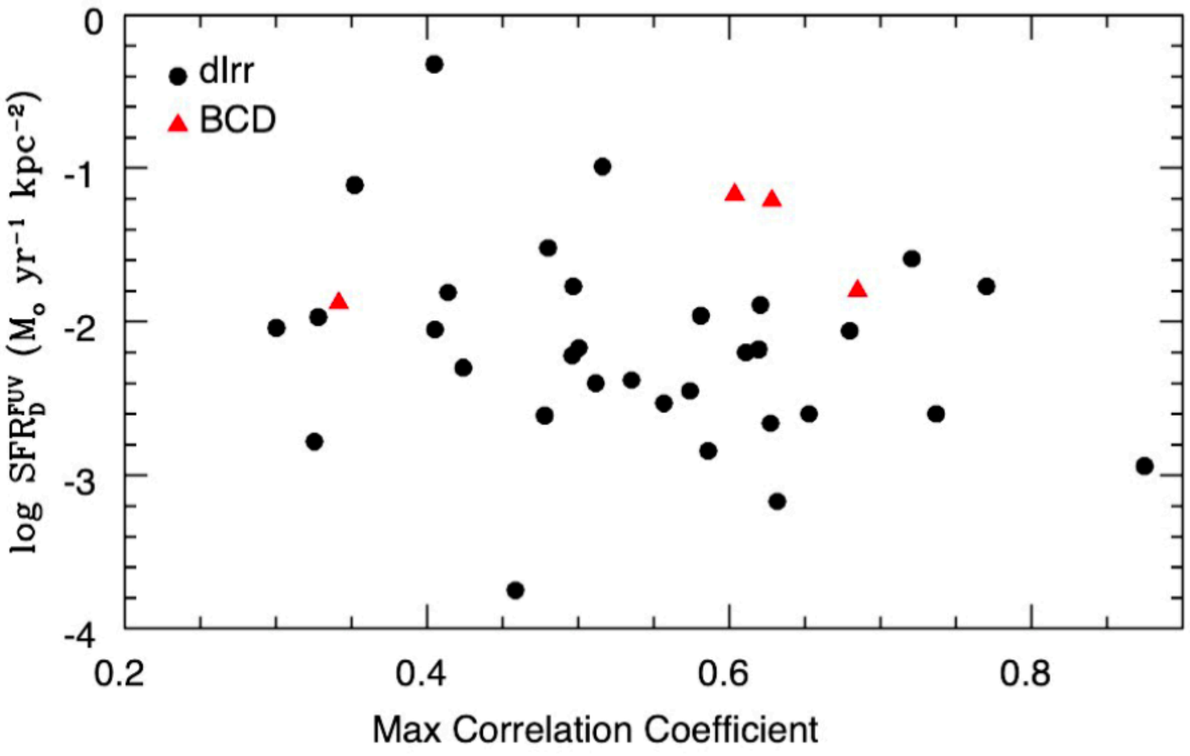

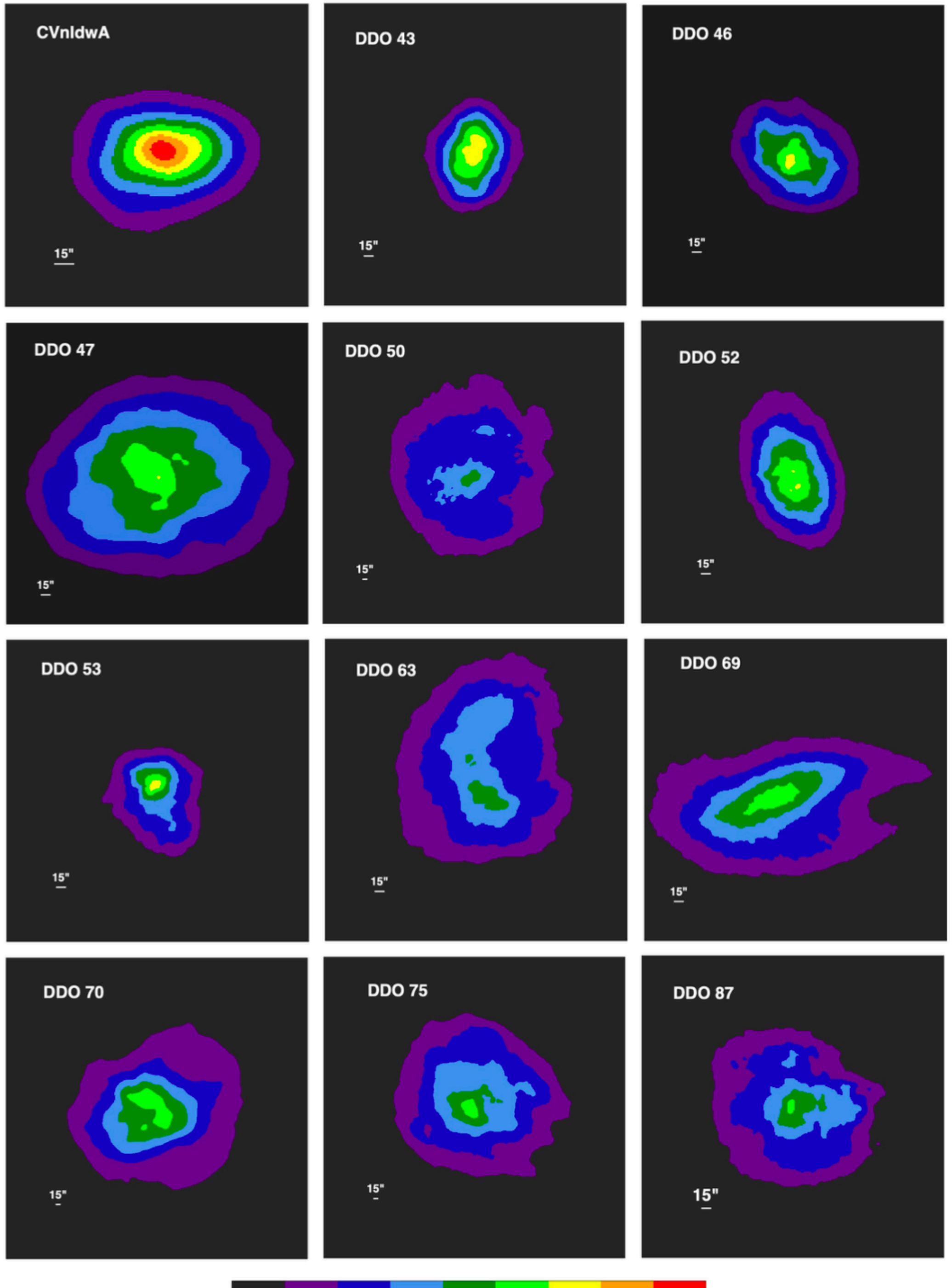

NGC2366

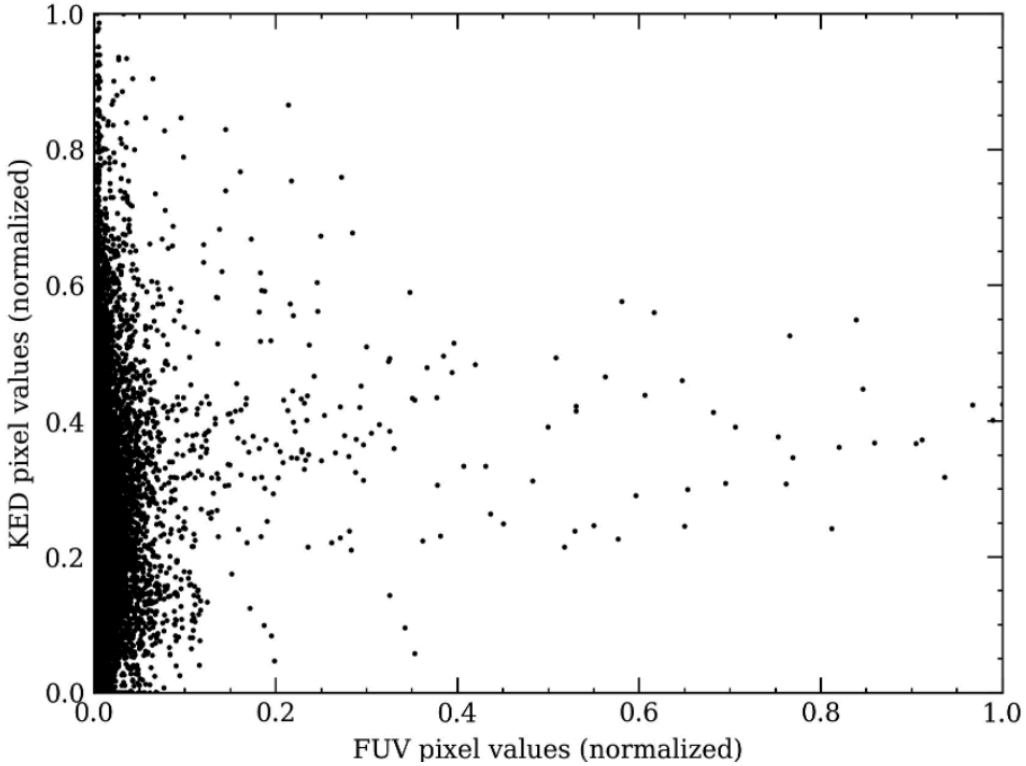

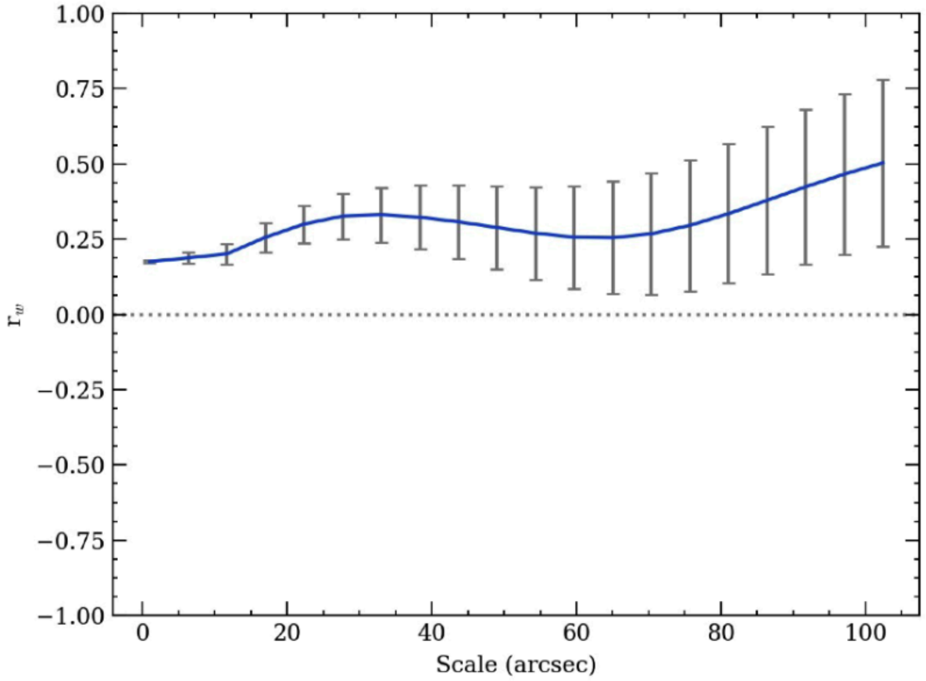

Fig. 3.— Cross-correlation coefficient r_w for NGC 2366 KED and FUV images convolved with progressively larger 'Mexican hat' kernels. We find no significant correlation between the two images at any resolved scale.

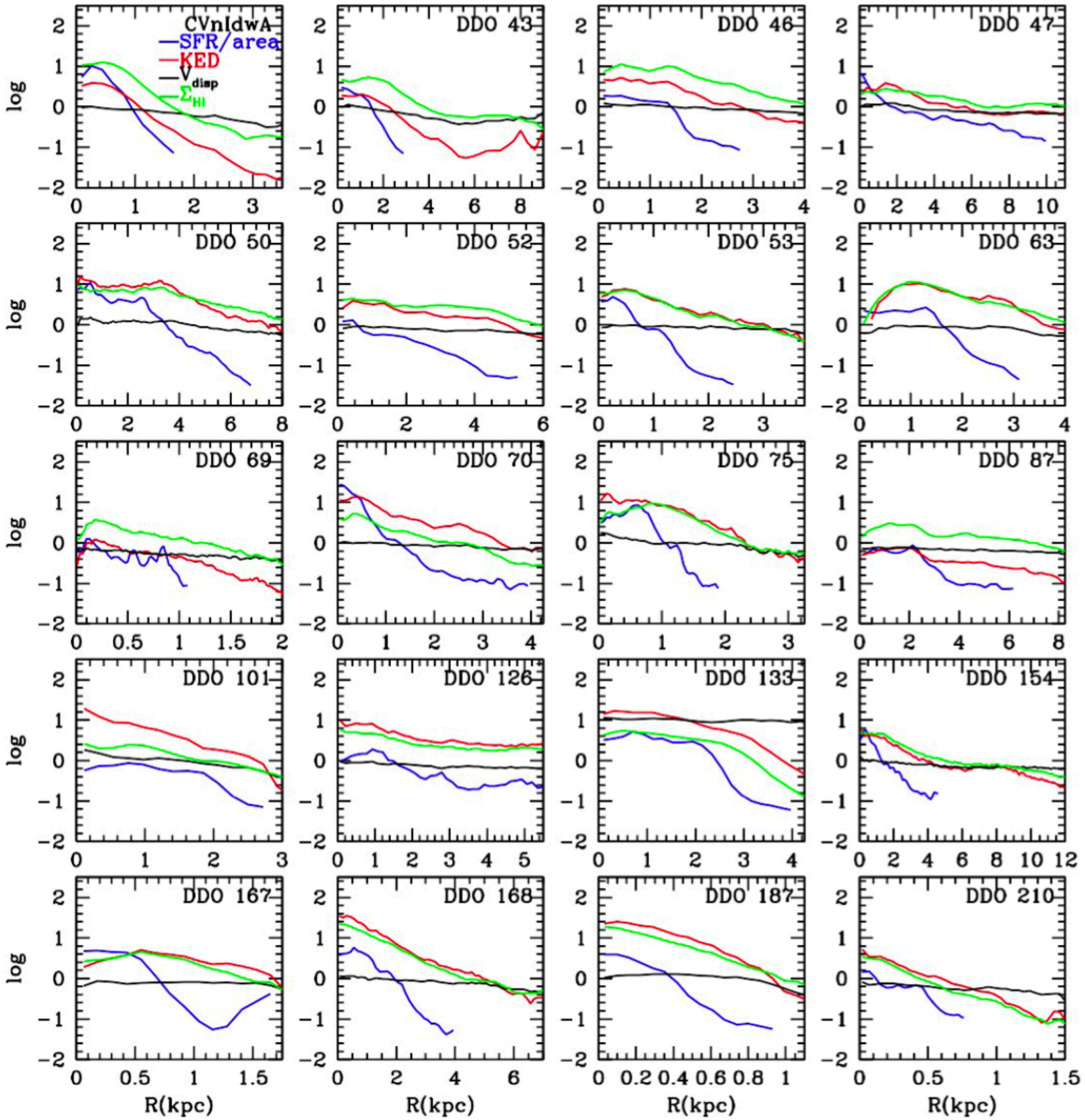

Fig. 10.— Azimuthally-averaged radial profiles of Σ_{SFR} determined from the FUV, KED (not corrected for He and heavy elements), v_{disp}, and Σ_{HI}. FUV emission is the limiting quantity in that it does not go out as far as the other quantities. Optical disk parameters (center, b/a, and major axis position angle) from Hunter et al. (2012) were used, and holes in the gas or FUV emission were not used in the averages.

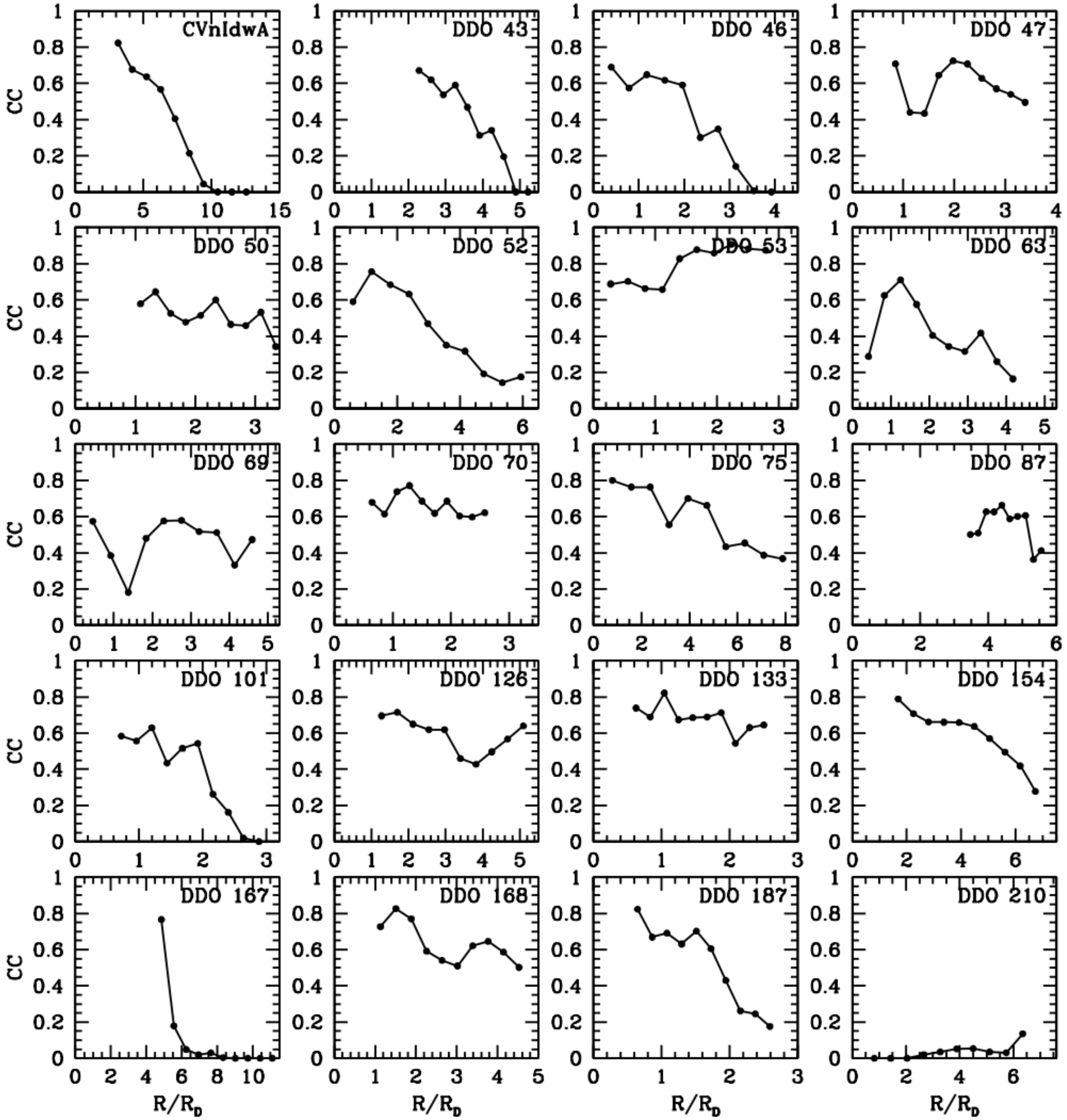

Fig. 5.— Correlation coefficient between FUV and KED images in annuli as a function of distance from the center of the galaxy. The C_{coef} profile is plotted from 0 to 1 for all galaxies for ease of comparison, and the radius is normalized by the disk scale length measured from the V-band image (Table 1). The pixel values in each annulus have been normalized by the average in the annulus, so large-scale trends with radius have been removed.

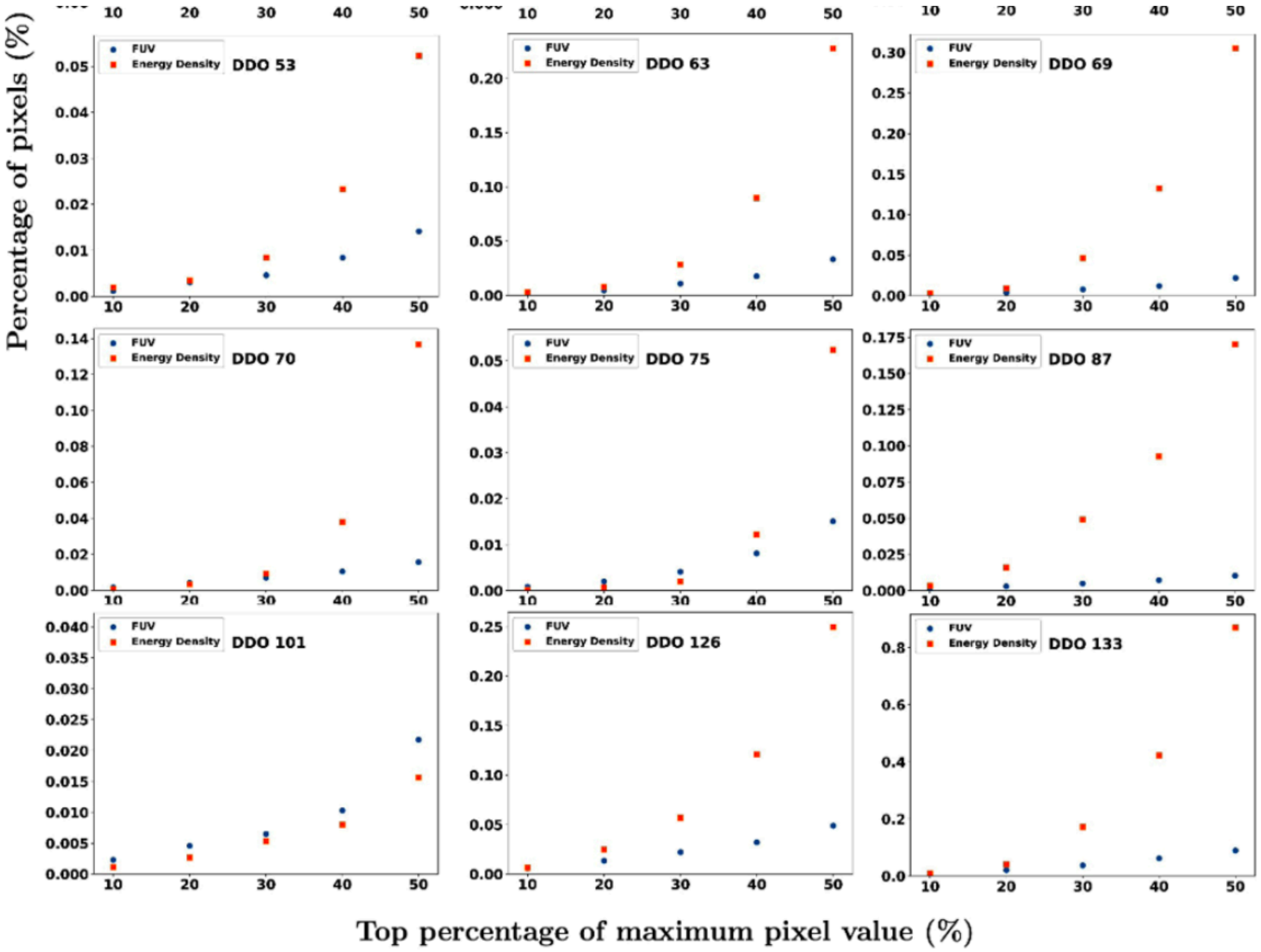

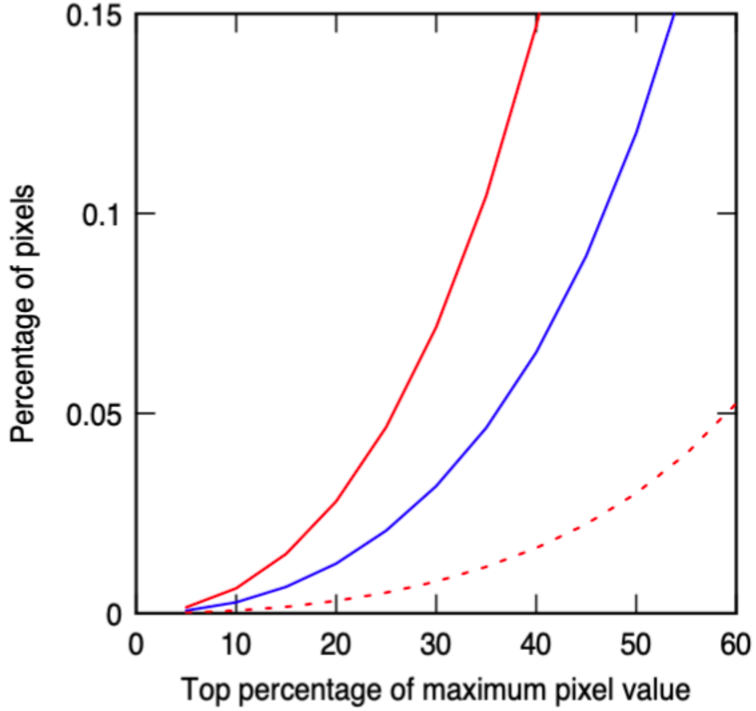

Fig. 8.— Percentage of pixels with values above a given percentage of the maximum value for FUV and KED images.

$$f(x) = \pi \left(-\ln[1-x]\right)^2 / \left(\pi r_{\rm max}^2\right)$$

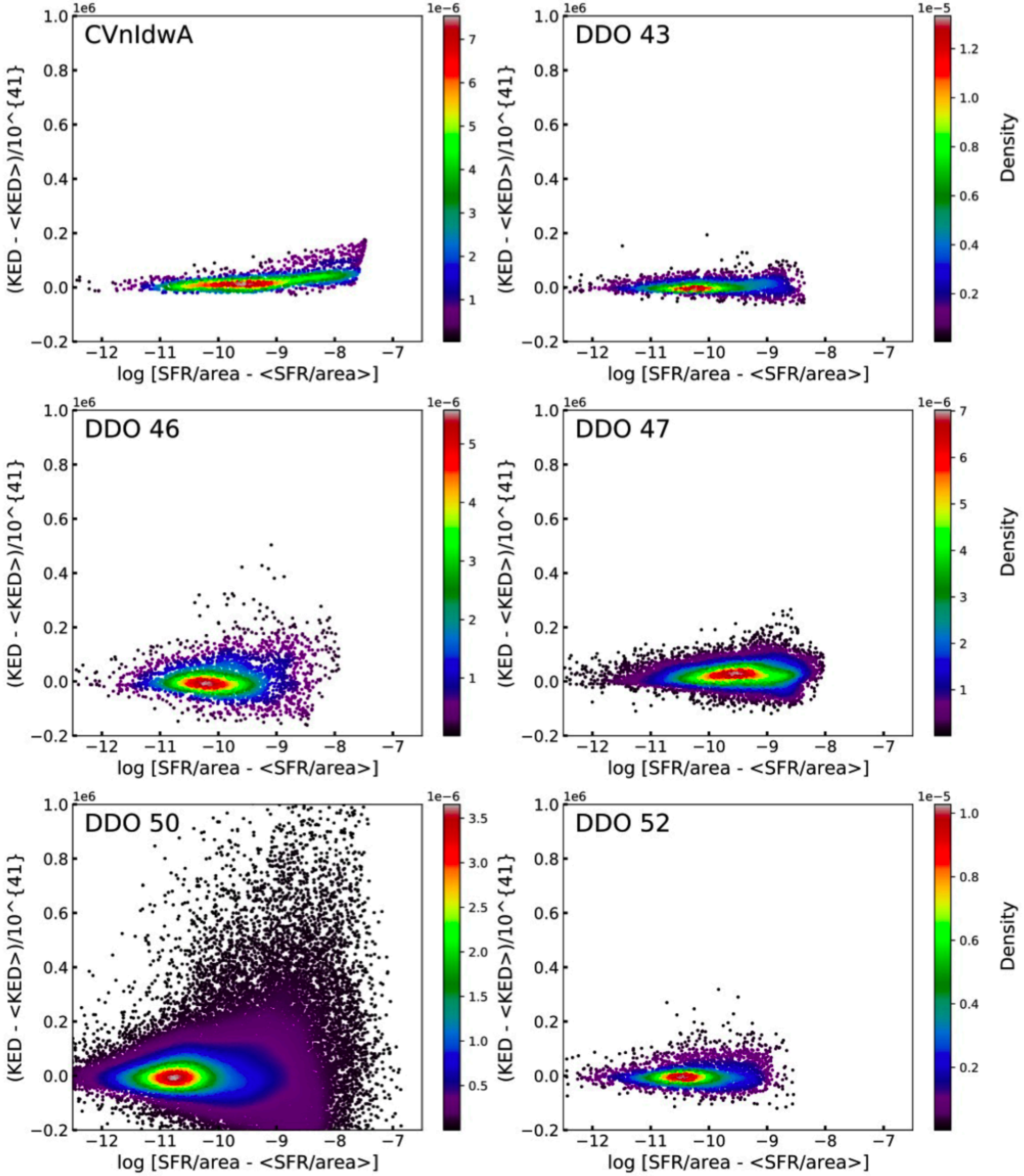

Fig. 11.— Pixel-pixel plots of the excess KED above the average value at each radius vs. the log of the excess $\Sigma_{\rm SFR}$. The density of points is color-coded. Figures for the rest of the galaxies in this study are available in the on-line materials (there are 6 figures like this for 36 galaxies). The KED has not been corrected for He and heavy elements.

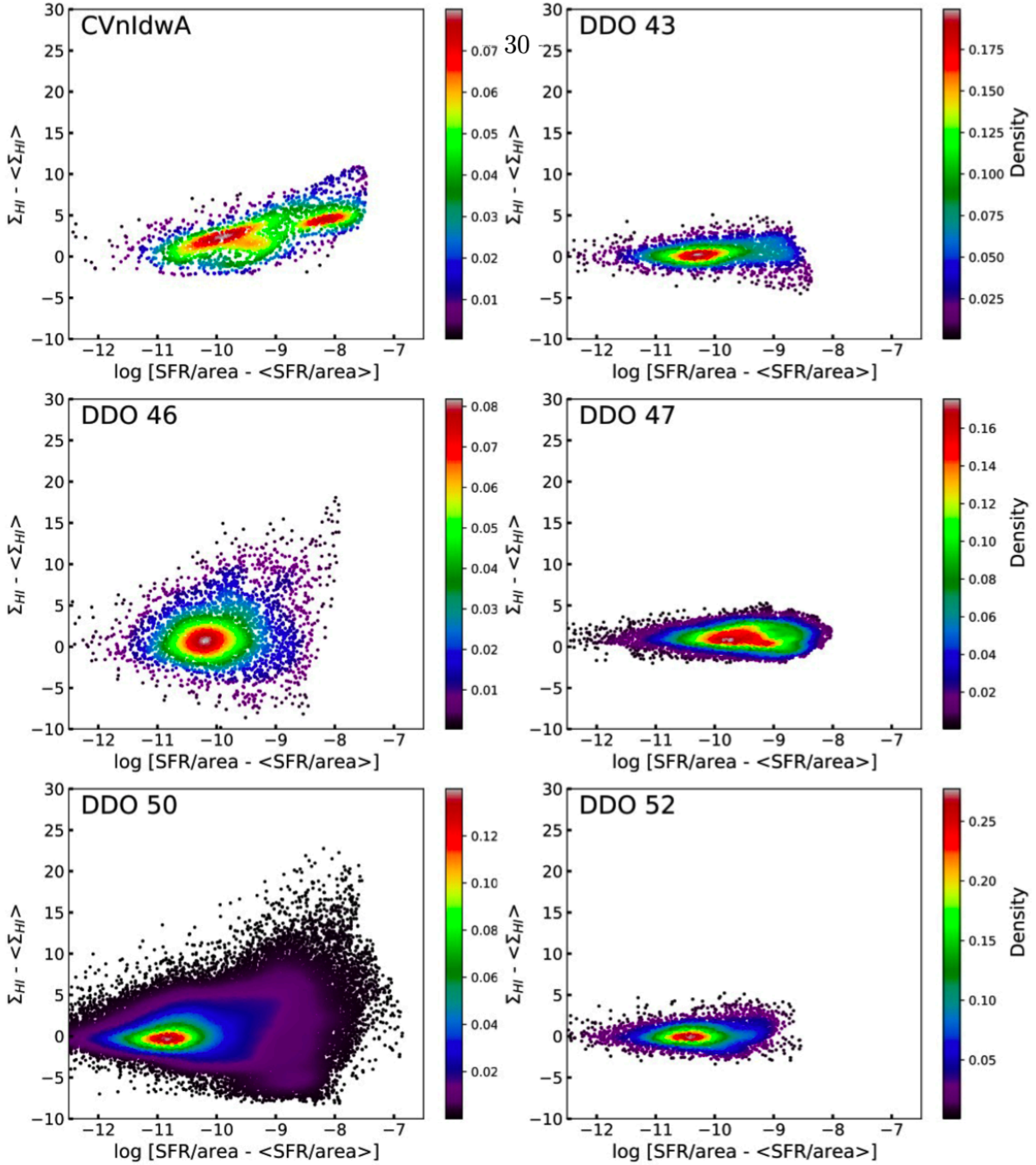

Fig. 13.— Pixel-pixel plots of the excess $\Sigma_{\rm HI}$ above the average value at each radius vs. log of the excess $\Sigma_{\rm SFR}$. The density of points is color-coded. Figures for the rest of the galaxies in this study are available in the on-line materials (the remaining 36 galaxies are shown in 6 figures).

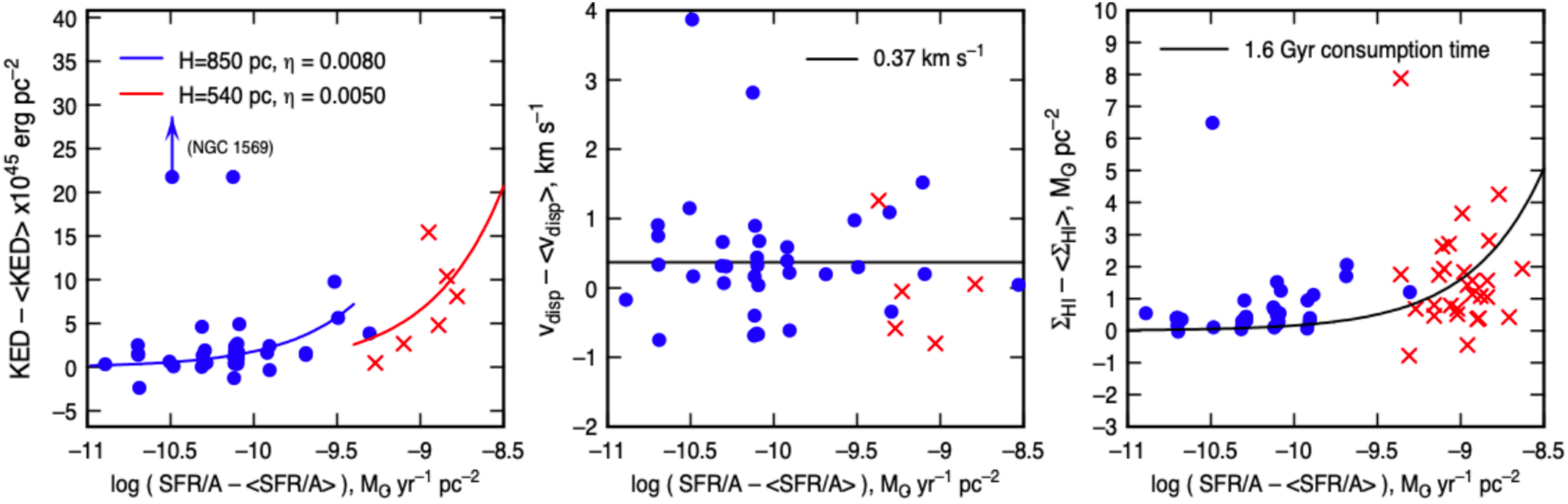

$$KED_{\rm SN} = \eta \Sigma_{\rm SFR} f_{\rm cc} E_{\rm SN} (2H/v_{\rm turb})$$

Bacchini et al. (2020): требуется хотя бы η = 1.5% для того, чтобы объяснить турбулентные движение действием лишь фидбэка от сверхновых

LITTLE THINGS: Удается согласовать лишь если η ~ 0.5%

Время исчерпания газа для HI в карликах сопоставимо с тем, что получается для молекулярного газа в больших галактиках (2 Gyr => Bigiel+ 2008)